Int. J. Nanosci. Nanotechnol., Vol. 13, No. 1, March. 2017, pp.69-82

Synthesis, Structure, Spectroscopy and Photocatalytic Studies of Nano Multi-Metal Oxide $MgO{\cdot}Al_2O_3{\cdot}ZnO$ and $MgO{\cdot}Al_2O_3{\cdot}ZnO$-Curcumin Composite

Md Abdus Subhan[1]∗, Pallab Chandra Saha[1], Nizam Uddin[1] and Prosenjit Sarker[2]

[1]Department of Chemistry, Shah Jalal University of Science and Technology, Sylhet, Bangladesh
[2]Square Pharmaceuticals Ltd., Bangladesh

(*)Corresponding author: subhan-che@sust.edu
(Received: 25 May 2016 and Accepted: 7 November 2016)

Abstract

The mixed metal nanocomposite $MgO{\cdot}Al_2O_3{\cdot}ZnO$ has been prepared by coprecipitation method. The product was characterized by XRD. The average particle size was found to be 34.89 nm from XRD data. SEM and SEM-EDS were studied for evaluating surface morphology and elemental composition. The FTIR spectrum of prepared mixed metal nanocomposites $MgO{\cdot}Al_2O_3{\cdot}ZnO$ and $MgO{\cdot}Al_2O_3{\cdot}ZnO$-curcumin were studied. The optical properties of the nanocomposites were studied by PL (Photoluminescence). The quantum efficiency (Φ) of $MgO{\cdot}Al_2O_3{\cdot}ZnO$ and $MgO{\cdot}Al_2O_3{\cdot}ZnO$-curcumin was found to be 0.86 and 0.31, respectively in acetone. The photocatalytic activity of the nano composite, $MgO{\cdot}Al_2O_3{\cdot}ZnO$ was investigated over methyl violet 6b (MV) dye under UV-Visible light irradiation. The photocatalytic activity was assessed with various parameters including variation of pH, effect of H_2O_2 and reusability. The dye degradation efficiency of nanocomposite was observed to be 48.7% and 93.42% for catalyst and catalyst with H_2O_2 at pH 9. The efficiency was 86.96% for catalyst with H_2O_2 at pH 7.

Keywords: *Nanostructures, Catalytic Properties, Luminescence, Optical Materials, Semiconductors.*

1. INRODUCTION

Mixed metal oxides have fascinating optical, electrical, magnetic, adsorbent, catalytic and chemical properties, which are not typically observed in the single individual components [1-7]. Metal oxides represent one of the most important and widely engaged categories of solid state catalysts either as active phases or as supports [8]. It has versatile uses in many areas of science like Chemistry, Physics, Material Science and Environmental Science [9]. Metal oxides are expected to replace and alter silicon and metal nitride based expensive electronic devices and ICs. Different applicable parameters of metal oxide arise due to its versatile combination rendering the materials interesting in nanoelectronic devices, catalysis, nonlinear optical devices, sensors and so on [10]. Magnesium oxide (MgO) is important oxide materials that are used in many applications such as catalysis, catalyst supports, toxic wastes remediation, refractory materials and adsorbents [11]. Magnesium oxides are used as destructive adsorbents for toxic chemical agents [12]. Multi-metal oxides containing aluminium have also been found to have several applications in catalysis [13]. Zinc oxide (ZnO) is an exclusive material that has encouraged a vast amount of research in different areas. It is a wide-bandgap semiconductor with the bandgap energy of 3.3eV. It has potential as a luminescent material because the binding energy of exciton is 60 meV which is higher than

that of the other semiconductors [14–18]. The mixing of several metal oxides causes modification in the electronic structure of the system. This change also includes surface properties. Bulk electronic structure, the band gap, Fermi level position, transport properties, and so forth are affected mostly in the case of compounds and solid solutions. Surface properties are expected to be influenced by new boundaries between grains of different chemical compositions. It is anticipated that these entire phenomenon in an assembled system will contribute advantageously to the photocatalytic/catalytic mechanism [19]. There have been studies on nanoparticles coated with bioactive compounds [20-21]. Very recently we also have been interested in chemistry of curcumin, a very important bioactive dye. This dye has promising applications as anti-cancer and anti-alzeimers [22]. We have fabricated a composite of curcumin with $MgO{\cdot}Al_2O_3{\cdot}ZnO$ and characterized by IR and PL spectra. This paper focused on structure, spectroscopy and photocatalytic activities of mixed metal nanocomposite $MgO{\cdot}Al_2O_3{\cdot}ZnO$ prepared by a simple co-precipitation method as well as study of $MgO{\cdot}Al_2O_3{\cdot}ZnO$-curcumin composite.

2. MATERIALS AND METHOD

2.1. Materials

All the materials used for the research work were reagent grade and collected from Sigma-Aldrich. The XRD measurements were performed with Bruker-AXD advance laboratory diffractometer, using a Cu Kα. The diffraction patterns were recorded in the step scan mode at 0.05 steps and at a measurement rate of 10 s/step. The diffraction patterns were registered within the 2θ angle range from 20° to 90°. The morphology of the multi metal oxide particle, $MgO{\cdot}Al_2O_3{\cdot}ZnO$ was investigated with a scanning electron microscope, Hitachi S-4800 Scanning Electron Microscope (SEM). Samples for the SEM were prepared by dispersing the multi metal oxide on a carbon tape. The SEM images of the sample with different magnification were taken with 5 and 15.3 mm working distances by applying an accelerating voltage of 20 kV and current of 20 µA. Thermo Electron Corporation - NORAN System SIX microanalysis system was used to perform the qualitative chemical analysis of the sample. Point-and-shoot analyses were employed to determine the presence and distribution of elements in the sample.

Infrared spectra were recorded on KBr pellets with an IR Spectrophotometer (model No-SHIMADZU IP Prestidge-21, FTIR Spectrophotometer, Japan) in the 4000-400 cm^{-1}. Double beam UV-visible spectrophotometer (UV-1800 Series, UV-Vis spectrophotometer, Shimadzu Corporation, Kyoto, Japan) was used for monitoring the spectroscopic measurements. Quartz cells of 1 cm path length were used as sample cell. Optical property of particles was measured by a Spectroflurophotometer (Shimadzu Corp. model RF-5301). Electric Muffle Furnace (Gallenkamp, Korea) was used for calcination of metal oxide composite. pH meter (model pH's-25, Shanghai Rex instrument factory, the people's republic of China) was used for measuring the pH of the experimental solution. Centrifuge machine (IEC SPINETTE centrifuge. DAMON/IEC Division) was used to remove the catalyst particles from the aliquot portion withdrawn each time during photocatalytic measurements.

2.2. Methods

2.2.1. Synthesis of $MgO{\cdot}Al_2O_3{\cdot}ZnO$

$MgO{\cdot}Al_2O_3{\cdot}ZnO$ metal oxide composite was synthesized by coprecipitation of their carbonates from the aqueous solution of the metal salts. Solutions of 0.25M $MgCl_2{\cdot}6H_2O$, $AlCl_3{\cdot}6H_2O$ and $Zn(CH_3COOH)_2{\cdot}2H_2O$ and a solution of 1M Na_2CO_3 in distilled water were prepared. $Zn(CH_3COOH)_2{\cdot}2H_2O$, $MgCl_2{\cdot}6H_2O$ and $AlCl_3{\cdot}6H_2O$ solutions

were mixed together in a beaker in 1:1:1 ratio and stirred vigorously at room temperature for five minutes. Then the solution of 1M Na_2CO_3 was added slowly with agitation, until precipitation was complete. The resultant mixture was stirred for a further 4 h at 60 ºC with constant stirring. After terminating the reaction, the white metal carbonate precipitate was separated from the solution by centrifugation, washed several times with deionized water and finally dried at 220 ºC in an oven. The obtained white precipitate was crushed in a mortar to make it amorphous. Then the amorphous powder sample was calcinated in muffle furnace at 900 ºC for 4 h. The calcinations converted the carbonates of the sample into their oxides. The process may happen by the following reactions.

$4(Zn^{2+} + CH_3COO^-) + 4(Na^+ + CO_3^{2-}) + HOH \rightarrow Zn_4(CO_3)_3(OH)_2 + CO_2 + 4(Na^+ + CH_3COO^-)$

$2(Al^{3+} + Cl^-) + (2Na^+ + 3CO_3^{2-}) \rightarrow Al_2(CO_3)_3 + 2(Na^+ + Cl^-)$

$(Mg^{2+} + Cl^-) + (Na^+ + CO_3^{2-}) \rightarrow MgCO_3 + (Na^+ + Cl^-)$

Calcination at 900 ºC:

$Zn_4(CO_3)_3(OH)_2 \rightarrow 4ZnO + H_2O + 3CO_2$

$Al_2(CO_3)_3 \rightarrow Al_2O_3 + 3CO_2$

$MgCO_3 \rightarrow MgO + CO_2$

2.2.2. Synthesis of $MgO{\cdot}Al_2O_3{\cdot}ZnO$-Curcumin Composite

For the synthesis of $MgO{\cdot}Al_2O_3{\cdot}ZnO$-curcumin composite 0.25 g of prepared $MgO{\cdot}Al_2O_3{\cdot}ZnO$ nanoparticle was taken in 15 mL ethanol: water solution (1:1) in 100 mL double-necked round-bottom flask and stirred for five minutes. Then 0.025 g of curcumin was dissolved in 15 mL ethanol: water solution (1:1). This solution was added slowly to the above $MgO{\cdot}Al_2O_3{\cdot}ZnO$ nanoparticle suspension in round bottomed flask and heated 40-50 ºC for 3 h with continuous stirring with teflon-coated magnetic stirring bar. An orange color product was formed. Then the final product was filtered and washed several times with distilled water. The product was dried over night at room temperature in a desiccator. This composite was partially soluble in acetone. The composite formation improved the solubility of $MgO{\cdot}Al_2O_3{\cdot}ZnO$ nanoparticle.

3. RESULTS AND DISCUSSIONS

3.1. X-Ray Diffraction Analysis

Fig. 1 shows the XRD pattern of $MgO{\cdot}Al_2O_3{\cdot}ZnO$. The diffraction peaks for the crystalline ZnO appear at 2θ angle of 31.43°, 34.29°, 36.53°, 47.37°, 56.25°, 62.72°, 67.72° and 68.72°. The diffraction peaks for crystalline MgO appear at 2θ diffraction angle of 31.47°, 42.49°, 56.25° and 62.72°. The diffraction angles (2θ) of 31.43°, 44.48°, 55.31°, 59.05°, 64.96°, 74.07° and 77.03° are due to the diffraction of crystalline $Al_2O_3{\cdot}ZnO$ (ICDD 00-005-0669). The crystallite sizes of the samples were calculated by using Scherrer's formula [23] $d = k\lambda / \beta \cos\theta$, where k (= 0.94) is the shape factor, d= average particle size, β is full width at half maxima (FWHM), θ is the Bragg angle, λ(=1.5406 Å) is the wavelength of Cu-Kα. The average particle size of $MgO{\cdot}Al_2O_3{\cdot}ZnO$ was found to be 34.89 nm.

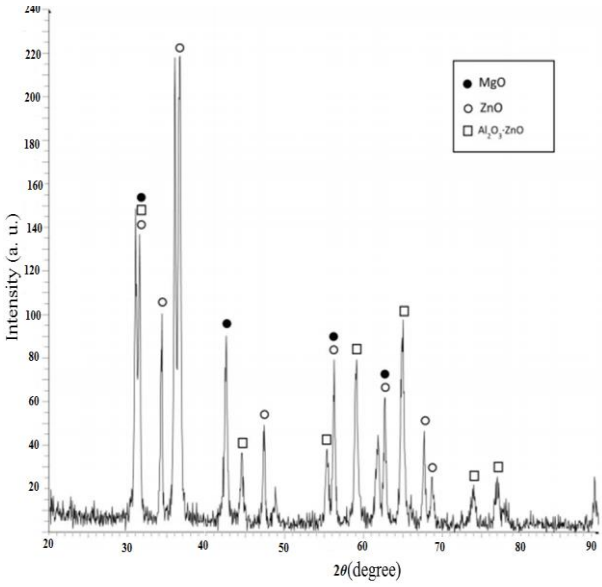

Figure 1*. X-Ray Diffraction pattern of $MgO{\cdot}Al_2O_3{\cdot}ZnO$ mixed metal oxide (closed*

circle, circle and square indicate peaks for MgO, ZnO and Al_2O_3·ZnO, respectively)

3.2. SEM and SEM-EDS Analysis

The SEM images of MgO·Al_2O_3·ZnO at different magnifications have been recorded. The SEM images of multi metal oxide nanocomposites were obtained to observe the particle size and morphology. A characteristic textures and morphology of MgO·Al_2O_3·ZnO have been revealed by the SEM study as shown in Fig. 2. SEM image showed that the sample contains three kinds of particles. The SEM image indicated that the annealed sample contains nanosized particles with hexagonal plates, small rod like and in some cases spherical morphology

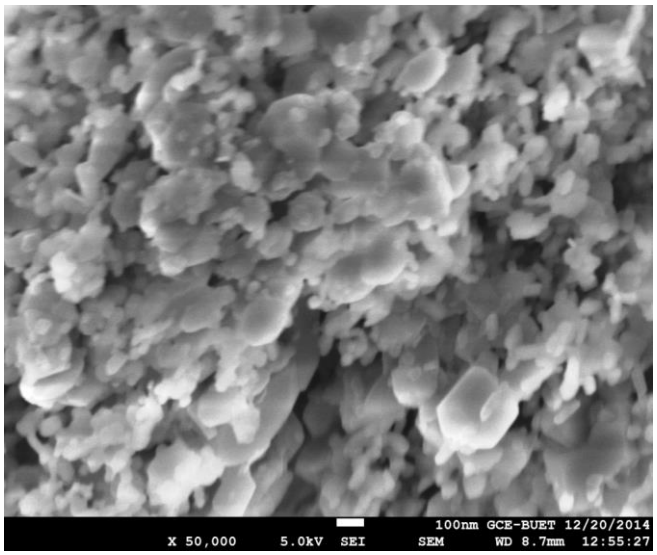

Figure 2*. SEM image of MgO·Al_2O_3·ZnO mixed metal oxide annealed at 900 ºC.*

EDS spectra showed that different parts of the sample (different measurement points in Fig.3) have an identical elemental composition of magnesium (Mg), aluminium (Al), zinc (Zn) and oxygen (O). Presence of elemental oxygen indicates the formation of metal oxides. Fig.3 shows an EDS spectrum measured from one point. On the basis of EDS result, metal oxides are dispersed at microscopic level in the nanocomposite. The atomic percentage of oxygen is comparatively small. The sample may contain some metal nano particles Mg, Al and Zn.

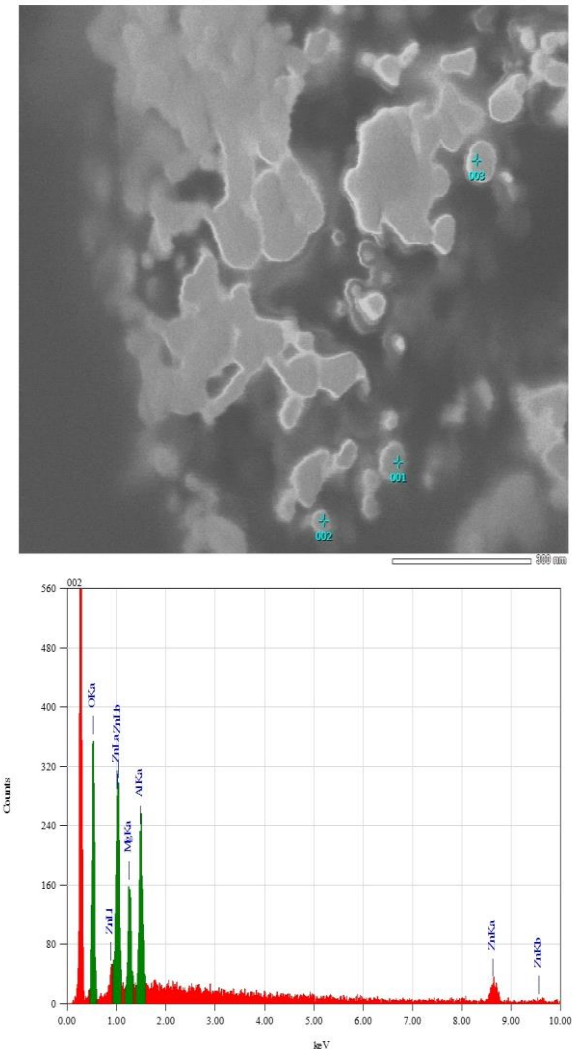

Element		(keV)	Mass%	Sigma	Atom%	C
O K		0.525	19.50	0.38	35.26	
Mg K	*	1.253	17.04	0.66	20.27	
Al K	*	1.486	26.02	0.82	27.90	
Zn L		1.012	37.44	1.00	16.57	
Total			100.00		100.00	

Figure 3. *SEM-EDS spectra of MgO·Al_2O_3·ZnO annealed at 900 ºC.*

3.3. FTIR Analysis of Curcumin and Composites

FTIR spectrum of curcumin (a) and MgO·Al_2O_3·ZnO-curcumin-composite (b) are as shown in figure 4. The bands observed centred at 3466 cm^{-1} and 1555 cm^{-1} are assigned to stretching and bending vibration of H_2O absorbed from the

environment [24], respectively for $MgO{\cdot}Al_2O_3{\cdot}ZnO$. The stretching mode of Zn-O bond appeared at 565 cm^{-1} [1]. The peaks observed at about 800-400 cm^{-1} indicating the formation of metal oxide (M-O) bonds. The IR peak at 518 cm^{-1} is due to Al_2O_3 particles which matched with the theoretical value calculated by DFT/B3LYP method [25] and peak observed at 696.8 cm^{-1} indicating the formation of Mg-O bond [26]. Fig. 4(a) shows the FTIR spectrum of curcumin in (KBr) at ν(cm^{-1}) 3510 (O-H), 1628 (C=O), 1510 (C=C), 1283 (C-O phenol), 1026 (C-O methoxy), 2847(C-H methyl ring), 3015 (aromatic ring), and 1000–1300 (C-O-C), characteristically ascribed to symmetric and asymmetric configurations of C–O–C chains. The IR spectrum of $MgO{\cdot}Al_2O_3{\cdot}ZnO$-curcumin composite shows peaks at ν(cm^{-1}) 3474(O-H), 1506(C=C), 1223(C-O phenol), 1026(C-O methoxy), 1000–1300 (C-O-C) [27]. From these IR spectra results it is thus evident that interactions of curcumin with $MgO{\cdot}Al_2O_3{\cdot}ZnO$ occurred through OH and C=O bonds in $MgO{\cdot}Al_2O_3{\cdot}ZnO$-curcumin composite because the IR peaks of OH and C=O either disappeared or red shifted (Fig 4 (b)).

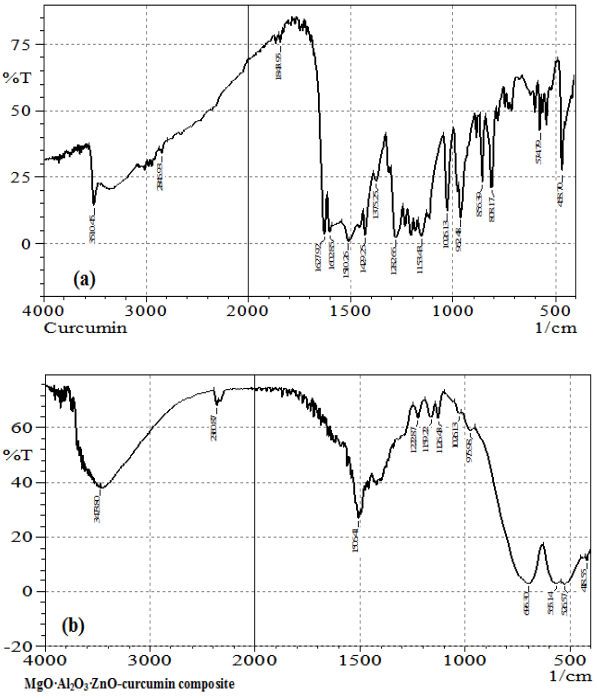

Figure 4. *(a) FTIR spectrum of curcumin and (b) $MgO{\cdot}Al_2O_3{\cdot}ZnO$-curcumin-composite.*

3.4. Photoluminescence Study

PL spectra of $MgO{\cdot}Al_2O_3{\cdot}ZnO$, curcumin and $MgO{\cdot}Al_2O_3{\cdot}ZnO$-curcumin composites were measured in acetone at room temperature at 220 and 330 nm excitations, respectively (Fig. 5 and table 1). When excited at 220 nm $MgO{\cdot}Al_2O_3{\cdot}ZnO$ nanoparticle shows a major peak at 372 nm. Corresponding to 330 nm excitation two PL peaks at 365 and 382 nm were also observed. Curcumin shows two emission peaks at 440 and 515 nm (green) for 220 nm excitation and another green PL peak at 515 nm when excited at 330 nm. The PL of $MgO{\cdot}Al_2O_3{\cdot}ZnO$-curcumin composites were also recorded at two different excitations. Excitation at 220 nm provided PL peaks at 368 and 512 nm (green). When excited at 330 nm $MgO{\cdot}Al_2O_3{\cdot}ZnO$-curcumin composite shows two emission peaks at 367 and 512 nm (green). PL spectra study clearly demonstrated that $MgO{\cdot}Al_2O_3{\cdot}ZnO$-curcumin composite provided PL peaks for both $MgO{\cdot}Al_2O_3{\cdot}ZnO$ at UV region (367-368 nm) and green PL of curcumin at 512 nm. The PL peaks of $MgO{\cdot}Al_2O_3{\cdot}ZnO$-curcumin composite is blue shifted compared to either $MgO{\cdot}Al_2O_3{\cdot}ZnO$ particle (original peak was observed at 372 nm) or curcumin (original peak was observed at 515 nm) as shown in Fig. 5 and table 1. This blue shift may be attributed to the formation of $MgO{\cdot}Al_2O_3{\cdot}ZnO$-curcumin composite by the attachment of curcumin on the surface of $MgO{\cdot}Al_2O_3{\cdot}ZnO$ nanoparticles. This was also evidenced by the FTIR study. The quantum efficiency (Φ) of the curcumin, $MgO{\cdot}Al_2O_3{\cdot}ZnO$ and $MgO{\cdot}Al_2O_3{\cdot}ZnO$-curcumin were measured in reference to anthracene in acetone at room temperature and found to be 0.11, 0.86 and 0.31 respectively. The excitation wavelength in

each case was 355 nm. The emission quantum yield of hybrid $MgO{\cdot}Al_2O_3{\cdot}ZnO$-curcumin is 31%, which is smaller than that of $MgO{\cdot}Al_2O_3{\cdot}ZnO$ (86 %), and which is larger than that of curcumin (11%). This may be due to some vibrational relaxation of excited state through C-H and C-O bonds present in curcumin.

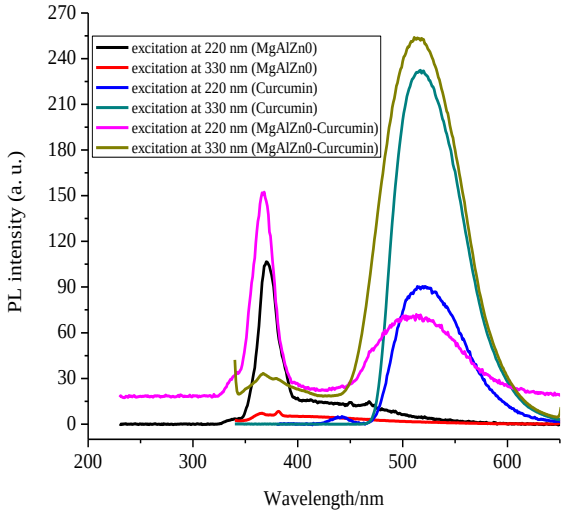

Figure 5. *PL spectra of $MgO{\cdot}Al_2O_3{\cdot}ZnO$, curcumin and $MgO{\cdot}Al_2O_3{\cdot}ZnO$-curcumin composite at different excitations.*

Table 1. *PL spectra data of curcumin and composites.*

Samples	Excitation Wavelength (nm)	Emissions Wavelength(nm)
$MgO{\cdot}Al_2O_3{\cdot}ZnO$	220	372
	330	365 and 382
Curcumin	220	440 and 515
	330	515
$MgO{\cdot}Al_2O_3{\cdot}ZnO$-curcumin composite	220	368 and 512
	330	367 and 512

Fig. 6 shows the excitation spectra of $MgO{\cdot}Al_2O_3{\cdot}ZnO$ nanoparticles, curcumin and $MgO{\cdot}Al_2O_3{\cdot}ZnO$-curcumin composite monitored at 540 nm in acetone. Two peaks at 350 and 440 nm are observed for $MgO{\cdot}Al_2O_3{\cdot}ZnO$. Curcumin shows excitation peak at 355 nm when monitored at 540 nm. A major peak at 449 nm was observed for $MgO{\cdot}Al_2O_3{\cdot}ZnO$-curcumin composite with two small peaks at 340 and 480 nm. This peak at 449 nm and others at 340 and 480 nm are corresponding to both $MgO{\cdot}Al_2O_3{\cdot}ZnO$ and curcumin transitions. The excitation spectra also clearly indicated the formation of $MgO{\cdot}Al_2O_3{\cdot}ZnO$-curcumin composite.

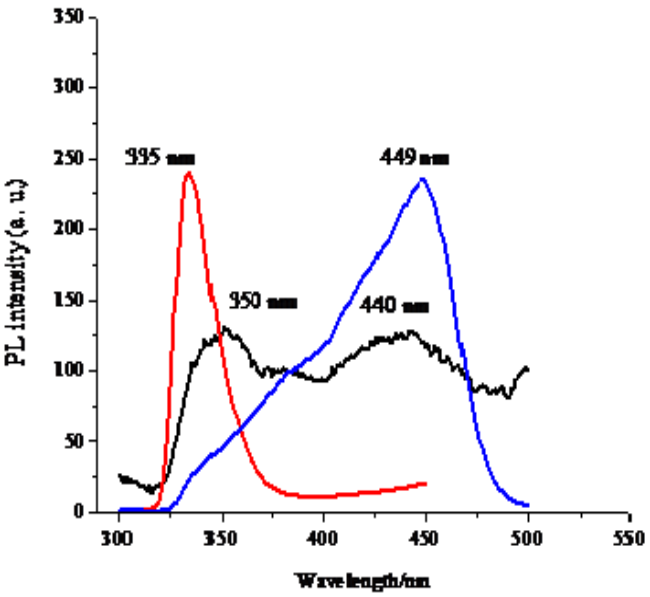

Figure 6. *Excitation spectra of $MgO{\cdot}Al_2O_3{\cdot}ZnO$ nanoparticles (black), curcumin (red) and $MgO{\cdot}Al_2O_3{\cdot}ZnO$-curcumin composite (blue) monitored at 540 nm.*

3.5. Evaluation of Photocatalytic Activity of $MgO{\cdot}Al_2O_3{\cdot}ZnO$

There have been studies on photo-catalytic degradation using metal oxide based catalysts [28-31]. The assembly of oxides MgO, Al_2O_3, ZnO in a composite may produce higher content of surface oxygen defects. The enrichment of surface oxygen defects, which can capture the photo-generated electrons and holes separately and make them available for decomposing organic contaminants is

considered to play an important role in the degradation of dyes and makes a major contribution to the enhanced photocatalysis [32]. The photocatalytic activity of the $MgO{\cdot}Al_2O_3{\cdot}ZnO$ composite was evaluated using degradation of Methyl Violet 6b dye under ambient conditions. The pH was adjusted with 0.1M HCl or 0.1M NaOH as required. The dye solution (100 ml, with initial concentration 5.0 ppm) was kept in a cylindrical Pyrex beaker of 5 cm diameter and 50 mg of catalyst ($MgO{\cdot}Al_2O_3{\cdot}ZnO$) and 30% of H_2O_2 (100 ml, 2.5 mM) were added into the dye solution. In order to ensure adsorption/desorption equilibrium, the solution was stirred for about 1 hour in dark, prior to the irradiation. The light source used was low-pressure mercury lamp (GERMEDICAL LAMP G-10T8) of 10W with wavelength 362 nm. The distance between experimental dye solution and light source was 25 cm. The reactor was set in an open air. 3 ml of solutions were collected at regular intervals and dye solutions were separated from the photo-catalyst by centrifugation before analysis. The change of concentration of dye solution was measured spectrophotometrically using Shimadzu-1800 double beam spectrophotometer. The photocatalytic efficiency (η) was calculated using the expression

$$\eta = (1-\frac{C}{C_0}) \times 100 = (1-\frac{A}{A_0}) \times 100 \qquad (1)$$

Where C_0 is the concentration of MV before irradiation and C is the concentration of MV after irradiation [33]. Photocatalytic activity of $MgO{\cdot}Al_2O_3{\cdot}ZnO$ was tested by irradiation of an aqueous suspension of methyl violet 6b (MV 6b) dye with 10 W low pressure mercury lamp. Fig. **7** (a-f) depicts the photocatalytic degradation of MV 6b dye in the presence of $MgO{\cdot}Al_2O_3{\cdot}ZnO$ nanocomposite at pH 9 and pH 7 respectively.

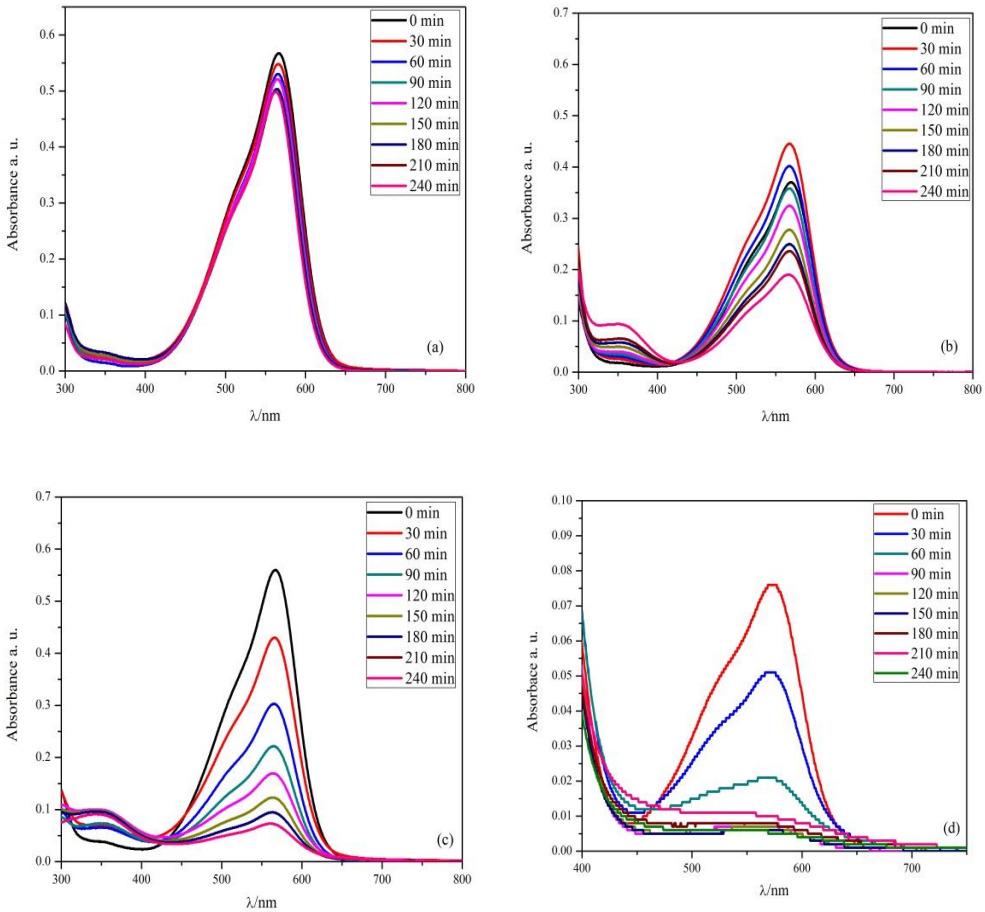

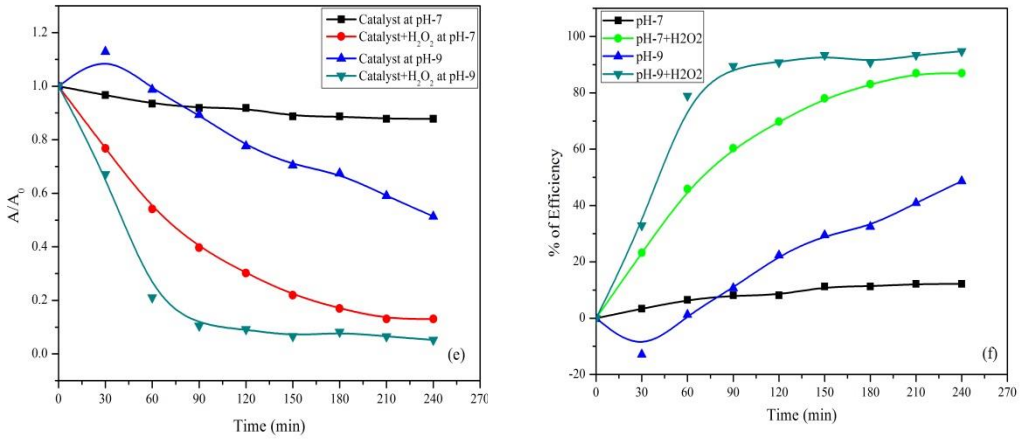

Figure 7. *Variation of the absorption spectrum of Methyl Violet 6b solution in the presence of $MgO{\cdot}Al_2O_3{\cdot}ZnO$ nanocomposite under UV light irradiation at different time intervals at (a) catalyst at pH 7, (b) catalyst at pH 9, (c) catalyst with H_2O_2 at pH 7, (d) catalyst with H_2O_2 at pH 9, (e) decrease in dye concentration with time at different conditions and (f) indicates the percentage of efficiency in the presence of catalyst and catalyst with H_2O_2 at pH 7 and pH 9.*

It has been found that the synthesized nanocomposite shows photocatalytic activity either in neutral (pH 7) or basic (pH 9) medium. Fig. **7** depicts the photocatalytic degradation of MV 6b dye at different pH values in the presence of $MgO{\cdot}Al_2O_3{\cdot}ZnO$ nanocomposite. It was found that the percentage of degradation yield were lower at neutral medium but higher at basic medium after 210 min of irradiation under UV light. Because at pH 9, the formation of hydroxyl radical (•OH) is favoured and the degradation yield is increased compared to pH 7 [34]. It was observed that the irradiation of aqueous suspensions of MV 6b dye in the presence of $MgO{\cdot}Al_2O_3{\cdot}ZnO$ nanoparticle leads to decrease in absorption intensity. It can be seen that the maximum absorbance of MV 6b at 570 nm gradually decreases with increasing irradiation time for $MgO{\cdot}Al_2O_3{\cdot}ZnO$. Fig. **7**(a) and (b) show the change in absorbance as a function of irradiation time for the MV 6b in the presence of catalyst at pH 7 and pH 9. Fig **.7** (c) and (d) also show the change in absorbance as a function of irradiation time for the MV 6b in the presence of catalyst with H_2O_2 at pH 7 and at pH 9. Fig. **7** (e) shows a plot for the degradation percentage *vs*. irradiation time (min) for the air saturated aqueous suspension of MV 6b in the presence of catalyst, catalyst with H_2O_2 at pH 7 and 9. Fig. **7** (f) shows that in the presence of catalyst at pH 7 and at pH 9, the degradation efficiency of 12.17% and 48.7% of MV 6b dye were observed, which were degraded after 210 min of irradiation time. However, it can be seen that in the presence of catalyst with H_2O_2 at pH 7 and pH 9, the efficiency of MV 6b dye degradation were 86.96 % and 93.42%, which were degraded after 210 min of irradiation time. When the $MgO{\cdot}Al_2O_3{\cdot}ZnO$ nanocomposite heterostructure is illuminated with UV light with photon energy higher or equal to the band gap of ZnO, electrons in the valence band (VB) can be excited to the conduction band (CB) leaving the corresponding holes in the valence band (VB). For pure ZnO, these photogenerated electrons and holes are easy to recombine within a time scale of nanoseconds [35]. For the $MgO{\cdot}Al_2O_3{\cdot}ZnO$ nanocomposite, its Fermi energy level (E_f) is lower than the energy level of the bottom of the CB of pure ZnO so the photo-excited electrons could transfer from ZnO nanoparticle to Mg or Al oxide nanoparticle. It has been proposed that a Schottky barrier formed at the interface between metal and

semiconductor, while the holes can remain on the semiconductor surfaces [36]. Therefore, Mg or Al nanoparticle on the surface of ZnO particles act as a sink for the electrons, promoting interfacial charge transfer kinetics between the metal and semiconductor and effectively hinder the recombination of photoexcited electrons and holes. Subsequently, the electrons can be captured by the soluble O_2 and the holes can be trapped by the surface hydroxyl ion, both resulting in the formation of hydroxyl radical species (•OH), which can rupture organic bonds and oxidize most of the pollutants. Similar mechanism has been proposed by Morales-Flores and Pal for photodegradation of phenol by Pt/ZnO nanocomposite [35]. The possible reason is that hydroxyl radicals are easily generated by oxidizing more hydroxide ions in alkaline solution, thus the efficiency of the process is logically enhanced at pH 9. Obviously, pH and H_2O_2 have strong effect on the photodegradation of dyes. When the addition of H_2O_2 to the heterogeneous system increases the concentration of •OH radicals as a result the percentage of dye degradation grows up. Being an electron acceptor, H_2O_2 does not only generate •OH radicals but it also inhibits the electron hole recombination process at the same time [33, 37]. As the concentration of •OH radicals become high, H_2O_2 consumes the excess of hydroxyl radicals and it performs like hydroxyl radical scavenger [33]. When H_2O_2 was added to the catalyst solution, the maximum degradation was achieved in the first 100 min. The complete degradation was achieved by 210 min. The methyl violet 6b (MV) is a cationic dye in aqueous solution whose optical spectrum remains invariant in the pH range 2.0 – 10.0 [38]. Therefore, any changes in the initial degradation yield caused by the variation of pH values must be ascribed to variation of the acid/base properties of the catalyst surface. It was seen that methyl violet 6b (MV) as a cationic dye is easily degraded in alkaline condition than in acid media [39]. So the photodegradation yield was higher at pH 9 than pH 7, which is correlated with the adsorption behaviour of dyes on the catalyst surface [40].

3.6. Kinetics Study

The reaction kinetics for the degradation of aqueous methyl violet solution (C = 5.0 ppm) using the UV–visible absorbance data was studied (Fig. 8). Fig. **7** (a-d) indicates that the concentration of methyl violet decrease linearly as a function of UV irradiation time. The kinetics of photocatalytic degradation of methyl violet on $MgO{\cdot}Al_2O_3{\cdot}ZnO$ dispersion under UV irradiation has often been performed with a simple Langmuir-Hinshelwood equation (Eq. (2)) [41].

$$r = -\frac{[MV]}{dt} = -\frac{kK[MV]}{1+K[MV]} \quad (2)$$

Where, r is the rate of disappearance of the reagent, [MV] is the reagent concentration, k is the rate constant, and K is the observed equilibrium constant.

The Langmuir-Hinshelwood equation can be simplified to a pseudo-first order expression if the concentration of reagent is very low ([MV] = 5 ppm).

$$r = -\frac{[MV]}{dt} = k_{obs}[MV] \quad (3)$$

Integration of Eq. (3) leads to Eq. (4)

$$\ln\left(\frac{[MV]_o}{[MV]}\right) = k_{obs}t \quad (4)$$

A plot of $\ln([MV]_0/[MV])$ vs. time produced a straight line with slope k (Fig. 8). Fig. 8 shows that the pseudo-first order assumption describes the experimental data well [42]. The observed dye degradation rate and the values of r-squared are listed in the table 2.

Table **2**: Values of rate constant (k) and r^2 for dye degradation kinetics of $MgO{\cdot}Al_2O_3{\cdot}ZnO$

Observation	k(min^{-1})	r^2
(a) Catalyst at pH 7	0.00053	0.8884
(b) Catalyst with H_2O_2 at pH 7	0.00912	0.98136
(c) Catalyst at pH 9	0.00313	0.93411
(d) Catalyst with H_2O_2 at pH 9	0.01157	0.77764

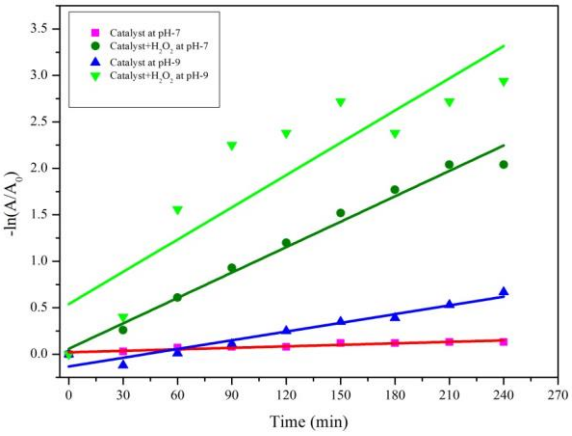

Figure. 8. *Natural logarithm of absorbance of methyl violet 6b plotted as a function of UV irradiation time (MV dye (5.0 ppm) degradation by MgO·Al₂O₃·ZnO (50 mg) in presence and absence of H_2O_2 at pH 7 and pH 9).*

3.7. Evaluation of Catalyst Stability

The possibility of catalyst recovery and reuse in photo-catalytic processes has received splendid interest. Since it can contribute significantly to lowering the operational cost of the process, which is an important parameter in the applicability of photo-catalysis as a method for industrial waste water purification. The regeneration of the catalyst can be done in a very simple way. After finishing the reaction, the solution was kept standing for 24 h and then the supernatant was decanted. The catalyst was thoroughly rinsed with distilled water and dried at 220 °C for 5 h. To evaluate reused photocatalyst efficiency, a series of experiments were performed using 0.5 g/L catalyst in presence of H_2O_2 and UV power of 10 W of the methyl violet 6b (dye) solution. The experimental results are shown in Fig. **9**. In the presence of catalyst with H_2O_2 at pH 9, the percentages of efficiency were 93.42%, 90.74%, 89.83% and 86.96% after 210 min of irradiation, respectively. As a result, the rate of degradation is still significant after four times of MgO·Al₂O₃·ZnO reuse. Agglomeration and sedimentation of the dye around MgO·Al₂O₃·ZnO particles after each cycle of photo-catalytic degradation is a possible cause of the observed decrease in the degradation rate, because each time the photo- catalyst is reused parts of the catalyst surface become unavailable for dye adsorption and thus photon absorption, reducing the efficiency of the catalytic reaction. The results showed that the catalytic activity of the catalyst-H_2O_2 at pH 9 has an apparent decrease in second reuse and subsequently maintained the relative stability.

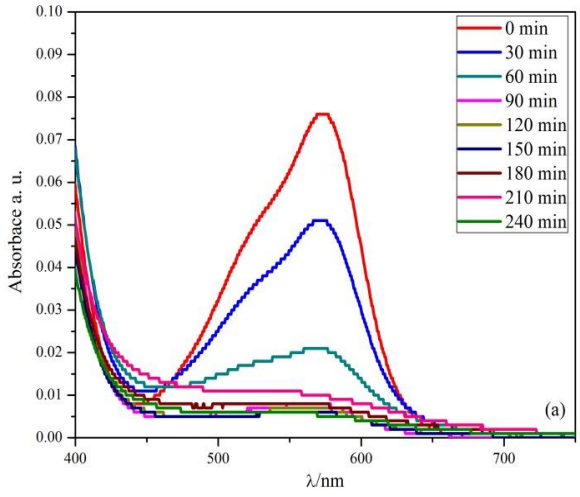

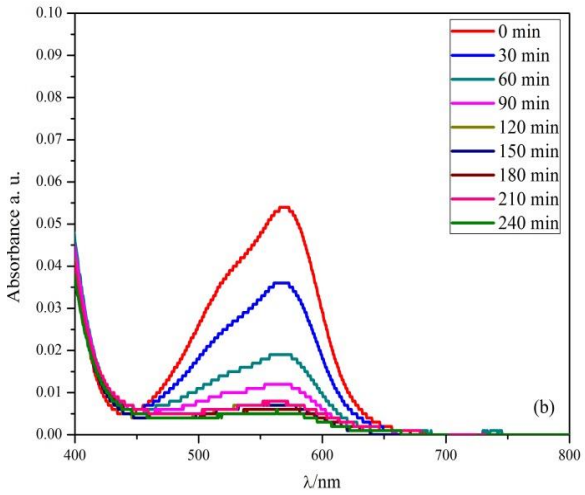

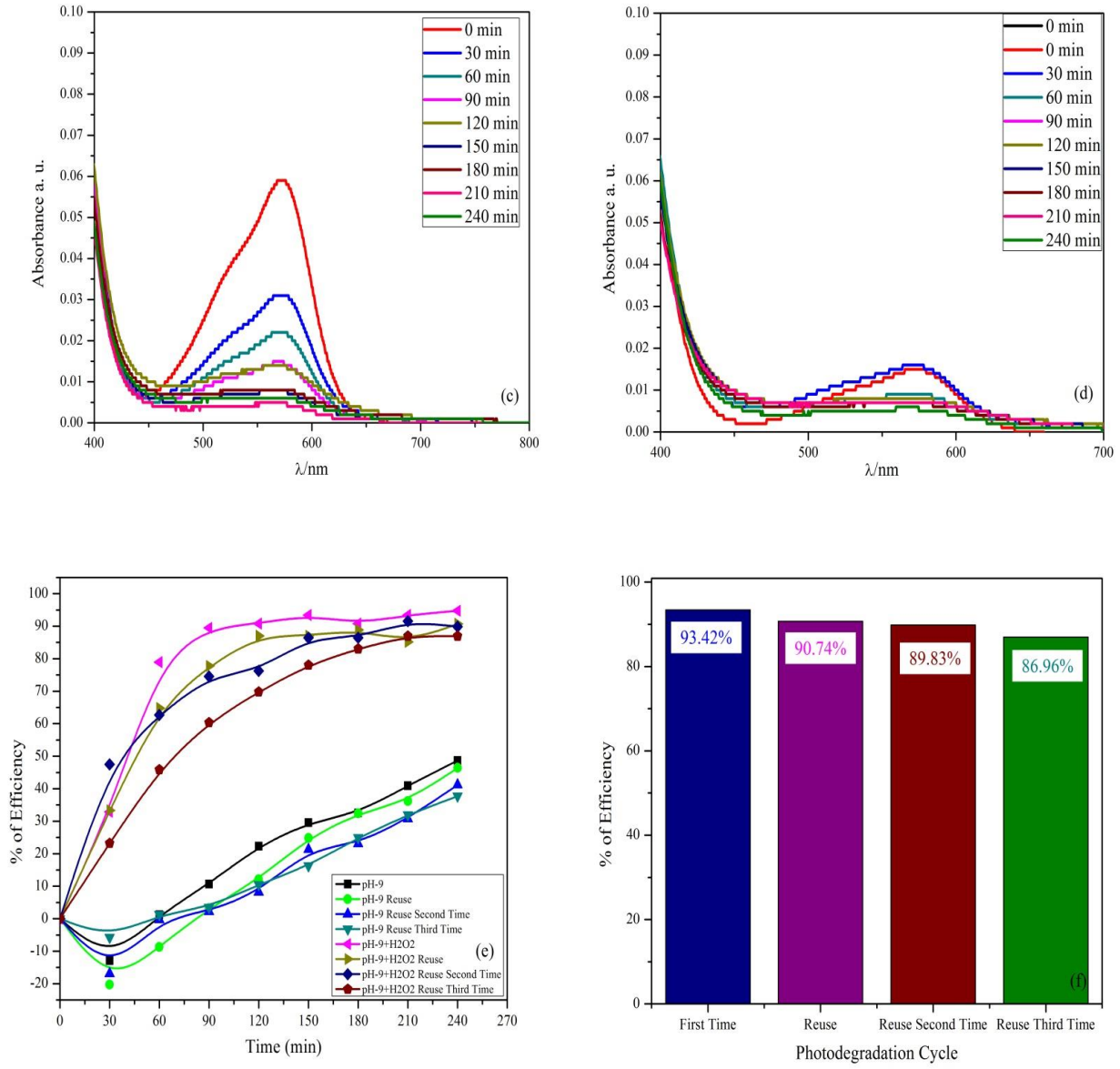

Figure 9. *The recycle and reuse of catalyst with H_2O_2 at pH 9 is represented in* ***(a)*** *Catalyst with H_2O_2 first time use,* ***(b)*** *Catalyst with H_2O_2 second time use,* ***(c)*** *Catalyst with H_2O_2 third time use,* ***(d)*** *Catalyst with H_2O_2 fourth time use,* ***(e)*** *Shows the combined efficiency of reusability of only catalyst and catalyst with H_2O_2 at pH 9 and* ***(f)*** *Shows the efficiency of reusability of catalyst with H_2O_2 at pH 9.*

4. CONCLUSION

Mixed metal oxide nanocomposite $MgO{\cdot}Al_2O_3{\cdot}ZnO$ was successfully synthesized by simple co-precipitation method. The prepared product was characterized by XRD, SEM, SEM-EDS PL and FTIR spectroscopy. The particle size was calculated by Scherrer's formula using XRD data and the average particle size has been found to be 38.89 nm. $MgO{\cdot}Al_2O_3{\cdot}ZnO$-curcumin composite was also fabricated and characterized by IR and PL. Both IR and PL spectra show strong evidence of interactions of curcumin with $MgO{\cdot}Al_2O_3{\cdot}ZnO$ in $MgO{\cdot}Al_2O_3{\cdot}ZnO$-curcumin composite. The quantum efficiency (Φ) of the curcumin, $MgO{\cdot}Al_2O_3{\cdot}ZnO$ and $MgO{\cdot}Al_2O_3{\cdot}ZnO$-curcumin were found to be 0.11, 0.86 and 0.31 respectively in acetone using anthracene as a standard. $MgO{\cdot}Al_2O_3{\cdot}ZnO$ and $MgO{\cdot}Al_2O_3{\cdot}ZnO$-curcumin showed different PL behaviour and may have important electronic properties. The photo-catalytic activity of synthesized composite $MgO{\cdot}Al_2O_3{\cdot}ZnO$ was tested on Methyl

Violet 6b dye in two different pH values along with various parameters including effect of H_2O_2 and reusability of catalyst. The highest photocatalytic efficiency of $MgO{\cdot}Al_2O_3{\cdot}ZnO$ was found to be 93.42% and 48.7% in the presence and absence of H_2O_2 at pH 9, respectively. The efficiency was 86.96% for catalyst with H_2O_2 at pH 7. The recycle and reusability efficiency of the synthesised nanocomposite was fascinating. Each component of trimetallic nanocomposite $MgO{\cdot}Al_2O_3{\cdot}ZnO$ is nontoxic, environmental friendly and may be a suitable photocatalyst for waste water treatment. $MgO{\cdot}Al_2O_3{\cdot}ZnO$-curcumin nanocomposite may also have important medicinal applications.

ACKNOWLEDGEMENT

TWAS research grant 2015 (No. 15-164 RG/CHE/AS_I – FR3240287058**)** is gratefully acknowledged for funding and travel grant to M.A. Subhan. MOE (Ministry of Education, Bangladesh) Grant 2015 is also acknowledged for another funding.

REFERENCES

1. Subhan M. A., Ahmed T., Sarker P., Pakkanen T. T., Suvanto M., Horimoto M. and Nakata H.,(2014). "Synthesis, structure, luminescence and photophysical properties of nano $CuO{\cdot}$ $ZnO{\cdot}$ $ZnAl_2O_4$ multi metal oxide" *J. Lumin.*, 148: 98
2. Terai Y., Yamaoka K., Yamaguchi T.and Fujiwara Y., (2009)."Structural and luminescent properties of Er-doped ZnO films grown by metalorganic chemical vapor deposition" *J. Vac. Sci. Technol.*, 27: 2248
3. Sun L., Hong X., Zou P., Chu X. and Liu Y., (2012). "Preparation and characterization of multifunctional Fe_3O_4/ZnO/SiO_2 nanocomposites"*J. Alloys Compd.*, 535: 91
4. Rodriguez J. A., Wang X., Hanson J. C., Liu G., JuezA. I. and Fernández-García M.,(2003). "The behavior of mixed-metal oxides: Structural and electronic properties of $Ce_{1-x}Ca_xO_2$ and $Ce_{1-x}Ca_xO_{2-x}$"*J. Chem. Phys.*, 119: 5659
5. Saleh R., Djaja N. F. andPrakoso S. P., (2013). "The correlation between magnetic and structural properties of nanocrystalline transition metal-doped ZnO particles prepared by the co-precipitation method" *J. Alloys Compd.*, 546: 48
6. Lu W., Sun D. and Yu H., (2013). "Synthesis and magnetic properties of size-controlled CoNi alloy nanoparticles" *J. Alloys Compd.*, 546: 229
7. Subhan M. A., Monim S. A., Bhuiyan M. B. R., Chowdhury A. N., Islam M. and Hoque M. A., (2011). "Synthesis, characterization of a multi-component metal oxide ($Al_{0.88}Fe_{0.67}Zn_{0.28}O_3$) and elimination of As (III) from aqueous solution*" Open J. Inorg. Chem.*, 2: 9
8. Manoj B. G., Rajesh K. P. and Radha V. J., (2012). "Role of mixed metal oxides in catalysis science versatile applications in organic synthesis"*Catal. Sci. Technol*., 2: 1113
9. JoseA. R. and Marcos, (2007). "Synthesis, properties, and applications of oxide nanomaterials"*Willey, New Jersey,* 4: 24
10. Li X., Fu J., Steinhart M., Kim D. H. and Knoll W., (2007). "Au/Titania Composite Nanoparticle Arrays with Controlled Size and Spacing by Organic-Inorganic Nanohybridization in Thin Film Block Copolymer Templates" *Bull. Korean Chem. Soc*., 6: 28
11. Mastuli M. S., Ansari N. S., Nawawi M. A., Mahat A. M., (2012). "Effects of cationic surfactant in sol-gel synthesis of nano sized magnesium oxide"*APCBEE Procedia,* 3: 93
12. Tenkgl V. S., Bakardjieva S., Marikova M., Bezdicka P., Subrt J., (2003)."Magnesium oxide nanoparticles prepared by ultrasound enhanced hydrolysis of Mg-alkoxides" *Matter. Letter*, 57:3998
13. Lu J., Tang Z., Zhang Z., Shen W., (2005). "Preparation of $LiFePO_4$with inverse opal structure and its satisfactory electrochemical properties" *Mater. Res. Bull.* 40: 2039
14. Huang M.H., Wu Y., Feick H., Tran N., Weber E., Yang P., (2001)."Catalytic Growth of Zinc Oxide Nanowires by Vapor Transport" *Adv. Mater.* 13: 113
15. Huang M. H., Mao S., Feick H., Yan H., Wu Y., Kind H., Weber E., Russo R., Yang P., (2001). "Room-temperature ultraviolet nanowire nanolasers"*Science,*292: 1897
16. VayssieresL., KeisK., HagfeldtA., LindquistS.E., (2001). "Three-Dimensional Array of Highly Oriented Crystalline ZnO Microtubes" *Chem. Mater.* 13: 4395
17. VayssieresL., (2003), "Growth of Arrayed Nanorods and Nanowires of ZnO from Aqueous Solution"*Adv. Mater.*15: 464

18. WangW., ZengB., YangJ., PoudelB., HuangJ., NaughtonM.J., RenZ., (2006).“Aligned ultralong ZnO nanobelts and their enhanced field emission” *Adv. Mater.* 18: 3275
19. ReddyB. M. and KhanA., (2005).“Recent Advances on TiO_2-ZrO_2 Mixed Oxides as Catalysts and Catalyst Support” *Catal. Reviews*, 47: 257
20. Zeinali S., Nasirimoghaddam S. and Sabbaghi S., (2016). “Investigation of the Synthesis of Chitosan Coated Iron Oxide Nanoparticles under Different Experimental Conditions”*Int. J. Nanosci. Nanotechnol*., 12 (3): 183
21. KurianM., VargheseB., AthiraT. S. and KrishnaS., (2016).“Novel and Efficient Synthesis of Silver Nanoparticles Using Curcuma Longa and ZingiberOfficinale Rhizome Extracts” *Int. J. Nanosci. Nanotechnol*., 12(3): 175
22. Wanninger S.,Lorenz V., Subhan A., Edelmann F. T., (2015).“Metal complexes of curcumin--synthetic strategies, structures and medicinal applications” *Chem. Soc. Rev.*, 44(15): 4986
23. SharmaA., Pallavi, Kumar S., (2012). “Synthesis and Characterization of CeO-ZnONanocomposites”*Nanoscience and Nanotechnology* 2(3): 82-85
24. ChuX. and ZhangH.,(2009). “Catalytic Decomposition of Formaldehyde on Nanometer Manganese Dioxide”*Mod. Appl. Sci*., 3: 175
25. MitinA.V.,(2011).“Accurate theoretical IR and Raman spectrum of Al_2O_2 and Al_2O_3 molecules”*StructChem,* 22: 411
26. Al-HazmiF., AlnowaiserF., Al-GhamdiA.A., Al-GhamdiAttieh A., AlyM. M., Al-TuwirqiR. M., and El-TantawyF.,(2012). “A new large – Scale synthesis of magnesium oxide nanowires: Structural and antibacterial properties”*Superlattices and Microstructures,* 52: 200
27. HatamieS., Nouri M., Karandikar S.K., Kulkarni A., Dhole S.D., Phase D.M. and KaleS.N.,(2012). “Complexes of cobalt nanoparticles and polyfunctional curcumin as antimicrobial agents”*Materials Science and Engineering C,* 32: 92–97
28. PeternelI. T., KoprivanacN., BozicA. M. and KusicH. M., (2007).“Comparative study of UV/TiO_2, UV/ZnO and Photo-Fenton processes for the organic reactive dye degradation in aqueous solution” *J. Hazard. Mater*., 148: 477
29. DaneshvarN., SalariD. and KhataeeA.R., (2004). “Photocatalytic degradation of azo dye acid red 14 in water on ZnO as an alternative catalyst to TiO_2”*Photochem. Photobio*., 162: 315
30. Roberts D. and MalatoS., (2002). “Solar photocatalysis a clean process for water detoxification” *The Sci. of the Total Environ*., 85: 291
31. AzamA., AhmedA. S., OvesM., KhanM. S., HabibS. S. and MemicA.,(2012). “Antimicrobial activity of metal oxide nanoparticles against Gram-positive and Gram-negative bacteria: a comparative study”*Int.J.Nanomed*., 7: 6003
32. SathishkumaraP., Sweenaa R., WubJ. J. and AnandanaS.,(2011). “Synthesis of CuO-ZnO nanophotocatalyst for visible light assisted degradation ofa textile dye in aqueous solution” *J. Chem. Eng*., 171: 136
33. SaravananR., KarthikeyanS., GuptaV. K., SekaranG., NarayananV. and Stephen A., (2013). “Enhanced photocatalytic activity of ZnO/CuO nanocomposite for the degradation of textile dye on visible light illumination” *J.Mater. Sci. Eng*., 33: 91
34. JalilpourM. and FathalilouM.,(2012). “Effect of aging time and calcination temperature on the cerium oxide nanoparticles synthesis via reverse co-precipitation method” *Int. J. Phy. Sci*., 7: 944
35. SubhanM. A., AhmedT., AwalR., Makioka R., NakataH.,PakkanenT. T., SuvantoM. and KimB. M.,(2014). “Synthesis, structure, luminescence and photophysical properties of nano $CuO{\cdot}ZnO{\cdot}ZnAl_2O_4$ multi metal oxide”*J. Lumin.*, 146: 123
36. RathodS., ArbadB. and LandeM.,(2010).“Preparation, characterization, and catalytic application of a nanosized $Ce_1Mg_xZr_{1-x}O_2$ solid heterogeneous catalyst for the synthesis of tetrahydrobenzo [b] pyran derivatives”*Chin. J. Catal*., 6: 631
37. MadhusudhanaN., YogendraK., Mahadevan K. M. and NaikS.,(2011). “Photocatalytic degradation of Coralene Dark Red 2B azo dye using calcium zincate nanoparticle in presence of natural sunlight: an aid to environmental remediation”*Int. J. Chem. Eng. Appl*., 2: 294
38. WangX. K., ChenG. H. and GuoW. L., (2003). “Sonochemical Degradation Kinetics of Methyl Violet in Aqueous Solutions”*Molecules.*, 8: 40.
39. JunjieL., ShiqingL., YuyangH., and JiaqiangW.,(2008). “Adsorption and degradation of the cationic dyes over Co doped amorphous mesoporous titania–silica catalyst under UV and visible light irradiation”*Microp. Mesop. Mater.*, 115: 416
40. Chu X. andZhangH., (2009). “Catalytic Decomposition of Formaldehyde on Nanometer Manganese Dioxide”*Mod. Appl. Sci*., 3: 175
41. S. Naskar, S. A. Pillay and M. Chanda,(1998). “Photocatalytic degradation of organic dyes in aqueous solution with TiO_2 nanoparticles immobilized on foamed polyethylene sheet”*J. Photochem. Photobiol. Chem. A*, 113: 257

42. KasanenJ., SalstelaJ., SuvantoM. and PakkanenT. T.,(2011). “Photocatalytic degradation of methylene blue in water solution by multilayer TiO_2 coating on HDPE”*Appl. Surf. Sci*., 258: 1738